
Chapter 5

TiO₂-ZrO₂ Composites

5.1 TiO₂-ZrO₂ Nanocomposites

Mixing of the oxides can produce new crystallographic phases with quite different properties than the original oxides [1]. The use of mixed oxides in many technological fields is an attractive strategy to produce materials with superior properties than the single components [2]. In particular, mixed oxides have been widely used in catalysis, because the surface characteristics of the individual oxides can be changed due to the formation of new sites in the interface between the components or by the incorporation of one oxide into the lattice of the other. It has been reported that incorporation of ZrO₂ into TiO₂ leads to decrease in particle size of TiO₂ and increase in surface area due to the dissimilar nuclei and co-ordination geometry [3]. A mixture of ZrO₂ and TiO₂ is used as an electrode for dye-sensitized solar cell [4].

5.2 Synthesis of Samples

A series of Titania–Zirconia mixed oxides with various TiO₂- ZrO₂ content (10, 30, 40, 60, 70 and 90 mol %) were prepared by the hydrothermal method. Titanium isopropoxide, Zirconium propoxide and isopropanol were used as starting chemicals. All chemicals were analytical grade and used as received. The synthesis was carried out as follows: Ti isopropoxide and Zr propoxide were diluted in isopropanol to obtain mixtures in a 1:9, 3:7, 4:6, 6:4, 7:3 and 9:1 ZrO₂:TiO₂ molar ratio. Dilute HNO₃ was added drop wise to the alkoxide solution kept under vigorous stirring in an ice bath. After alkoxide hydrolysis the alcogel was obtained. The alcogel was transferred to a stainless steel autoclave. The temperature was raised to 240 °C and the sample was maintained under autogenic pressure for 24 h.

Then, the sample was oven-dried at 100 °C (2 h) and finally calcined at 450 °C for 4 hours under static air atmosphere. Mixed oxides in solid form were obtained.

5.3 Characterization of Samples

The structural properties and composition of samples were analyzed by X-ray diffraction. The morphologies of the samples were analyzed with scanning electron microscope. The optical properties of the samples were investigated by UV-Visible spectroscopy.

5.3.1 X-Ray Diffraction Analysis

The XRD patterns were recorded on Bruker D8 Advance X-ray diffractometer in 2θ range of 20° to 90° at room temperature with a least count of 0.05° . The 2θ values are mentioned in degrees. The XRD patterns of samples are given in figures 1 to 6.

XRD pattern of Sample 1 (TiO₂-ZrO₂ composite in the ratio 9:1) shows broad and intense peaks which indicate formation of material in nano crystallite size with good amount of crystallinity. The presence of both oxides was confirmed from the comparison of d values with JCPDS data base (Anatase TiO₂: 21-1272, Rutile TiO₂: 21-1276, Monoclinic ZrO₂: 83-0944, Tetragonal ZrO₂: 79-1770). The experimental d values of all the peaks match very closely with JCPDS data. Eight peaks correspond to TiO₂ where as two peaks of ZrO₂ were observed in the pattern. Peaks at 2θ value of 25.35° , 37.4° , 47.9° , 62.5° and 75.1° correspond to Anatase phase of TiO₂ while those at 27.3° , 54.3° and 70° correspond to Rutile phase of TiO₂. Peak at 2θ value of 82.15° and 30.4° corresponds to Monoclinic and Tetragonal phase of ZrO₂ respectively. The mass fraction of Anatase phase is 50.39%.

Sample 2 (TiO₂-ZrO₂ composite in the ratio of 7:3) shows two phases each of TiO₂ (Anatase and Rutile) and ZrO₂ (Monoclinic and Tetragonal). The peak at 2θ value of 25.15° shows highest intensity and it is again the characteristic peak of crystal plane (101) of Anatase TiO₂. There are nine peaks corresponding to TiO₂ and five peaks corresponding to ZrO₂. Peaks at 2θ value of 25.15°, 37.4°, 47.9°, 53.75°, 62.5°, and 82.35° represent Anatase phase of TiO₂ where as peaks at 27.3°, 35.75° and 70° correspond to Rutile phase of TiO₂. Peaks at 41.15°, 50.65° and 54.8° represents Monoclinic phase of ZrO₂. Peaks corresponding to Tetragonal phase of ZrO₂ were observed at 30.4° and 74.75°. The structural parameters of sample are listed in Table 3. The Anatase content is 62.04%.

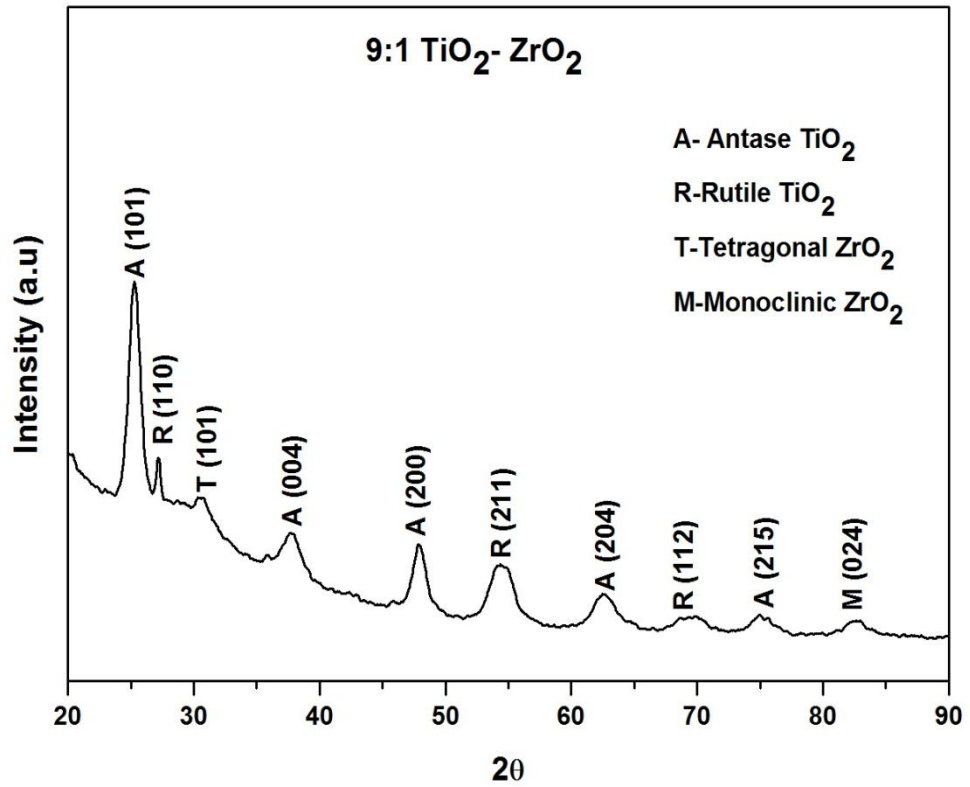
XRD pattern of sample 3 (TiO₂-ZrO₂ composite in the ratio of 6:4) has some sharp peaks with a hump in the initial range displaying some degree of amorphicity. The d values of all the peaks are closely matching with JCPDS data. TiO₂ is present in Anatase and Rutile phases where as only one phase i.e. monoclinic phase of ZrO₂ is present in the material. The peak at 2θ value of 25.30° is the characteristic peak of crystal plane (101) of Anatase TiO₂ and shows highest intensity. Six peaks corresponding to TiO₂ where as two peaks of ZrO₂ were observed in the pattern. Peaks at 2θ value of 25.30°, 37.4°, 47.9°, 53.75°, and 62.5° correspond to Anatase TiO₂ where as only one peak of Rutile TiO₂ has been observed at 27.3°. Peaks at 28.75° and 55.75° represent Monoclinic phase of ZrO₂. The intensities of peaks are relatively lower. The structural parameters of sample calculated from XRD pattern are given in Table 2. The Anatase mass fraction is 48.71%.

There are fewer peaks with comparatively low intensities in XRD pattern of sample 4 (TiO₂-ZrO₂ composite in the ratio of 4:6). This sample also exhibits some amorphicity. All other features are almost same as the other samples. The peak of

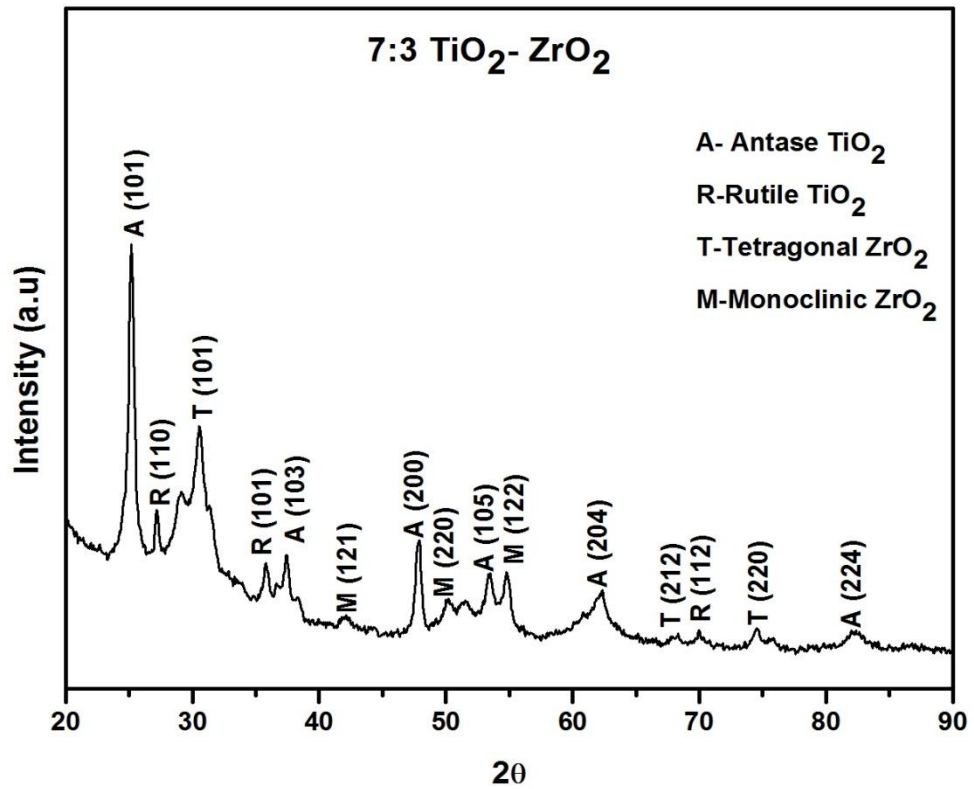
highest intensity at 25.25° corresponds to the characteristic peak of crystal plane (101) of Anatase TiO₂. There are seven peaks of TiO₂ and five peaks of ZrO₂. Peaks at 2θ value of 25.25°, 37.4°, 47.9°, 53.75°, 54.9° and 62.5° correspond to Anatase phase of TiO₂ where as only one peak corresponding to Rutile phase of TiO₂ is observed at 27.3°. Peaks at 28.35°, 70.2° and 74.8° represent Monoclinic phase of ZrO₂. Peaks corresponding to Tetragonal phase of ZrO₂ were observed at 68.75° and 82.55°. In this sample too, the intensities of peaks are relatively lower. The Anatase content is 52.88%. The structural parameters of sample are given in Table 4.

XRD pattern of sample 5 (TiO₂-ZrO₂ composite in the ratio of 3:7) again exhibits low crystallinity of sample with relatively low peak intensities. The d values of all the peaks closely match with JCPDS data. TiO₂ is obtained in Anatase and Rutile phase while ZrO₂ is only in Tetragonal phase. Two peaks corresponding to Anatase phase of TiO₂ were observed at 25.3° and 47.9°. Peak at 27.3° and 54.3° correspond to Rutile phase of TiO₂. Tetragonal phase of ZrO₂ was observed at 30.4°. The Anatase content is 41.99%. The structural parameters are listed in Table 5.

Broad peaks with good crystallinity are observed in Sample 6 (TiO₂-ZrO₂ composite in the ratio of 1:9). TiO₂ is present in only Rutile phase where as ZrO₂ is present in Monoclinic and Tetragonal phases. Most of the peaks correspond to Monoclinic ZrO₂. The peak at 2θ value of 24.50° has the highest intensity and is characteristic peak of crystalline plane (101) of Tetragonal ZrO₂. The structural parameters are listed in Table 6.

Figure 1: XRD pattern of sample 9:1 TiO₂-ZrO₂ compositeTable 1: Structural parameters of 9:1 TiO₂-ZrO₂ composite

Experimental d values	JCPDS d values	Crystallite size (nm)	Strain (%)	Anatase content (%)
3.5092	3.5200	5.26	0.047	50.39
3.2746	3.2400	5.11	0.045	
2.9087	2.9529	8.0	0.086	
2.3893	2.3780	24.69	0.026	
1.6831	1.6874	3.59	0.130	
1.4800	1.4804	6.89	0.054	
1.3432	1.3465	4.05	0.081	
1.2634	1.2649	4.8	0.059	
1.1707	1.1703	3.70	0.071	

Figure 2: XRD pattern of sample 7:3 TiO₂-ZrO₂ compositeTable 2: Structural parameters of 7:3 TiO₂-ZrO₂ composite

Experimental d values	JCPDS d values	Crystallite size (nm)	Strain (%)	Anatase content (%)
3.5366	3.5200	18.17	0.038	
3.2805	3.2400	24.23	0.026	
2.9227	2.9529	4.88	0.117	
2.5086	2.5380	17.99	0.027	
2.4016	2.4310	17.37	0.027	62.04
1.8968	1.8920	16.74	0.022	
1.7107	1.6999	16.25	0.020	
1.6731	1.6752	17.33	0.018	
1.4871	1.4808	4.52	0.064	

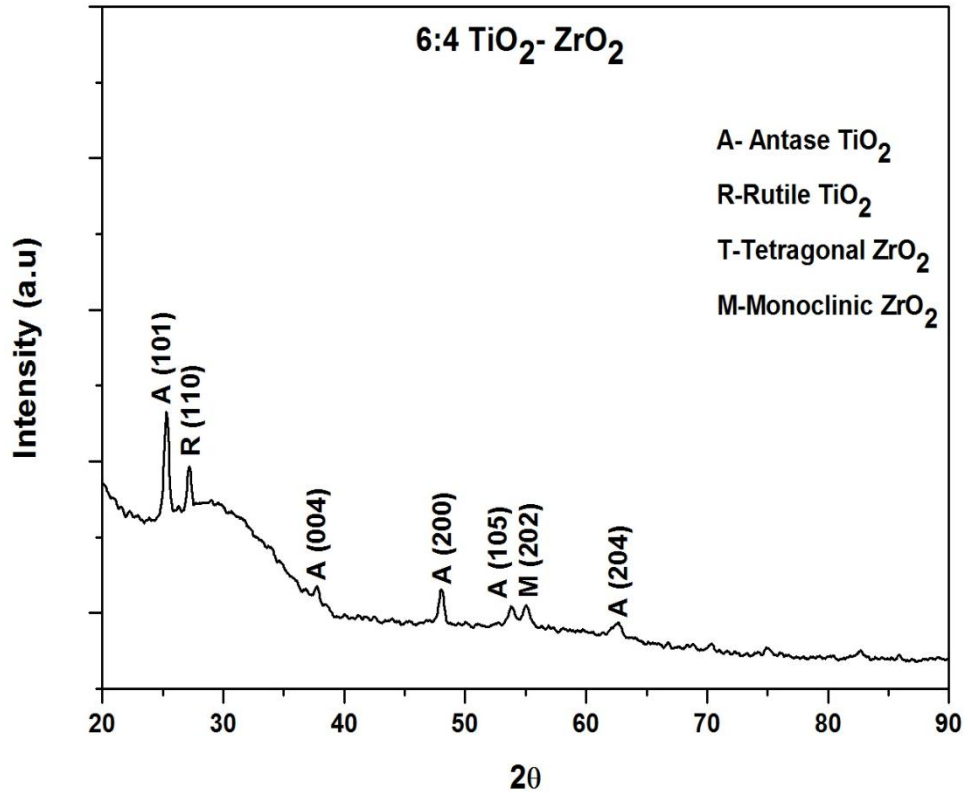
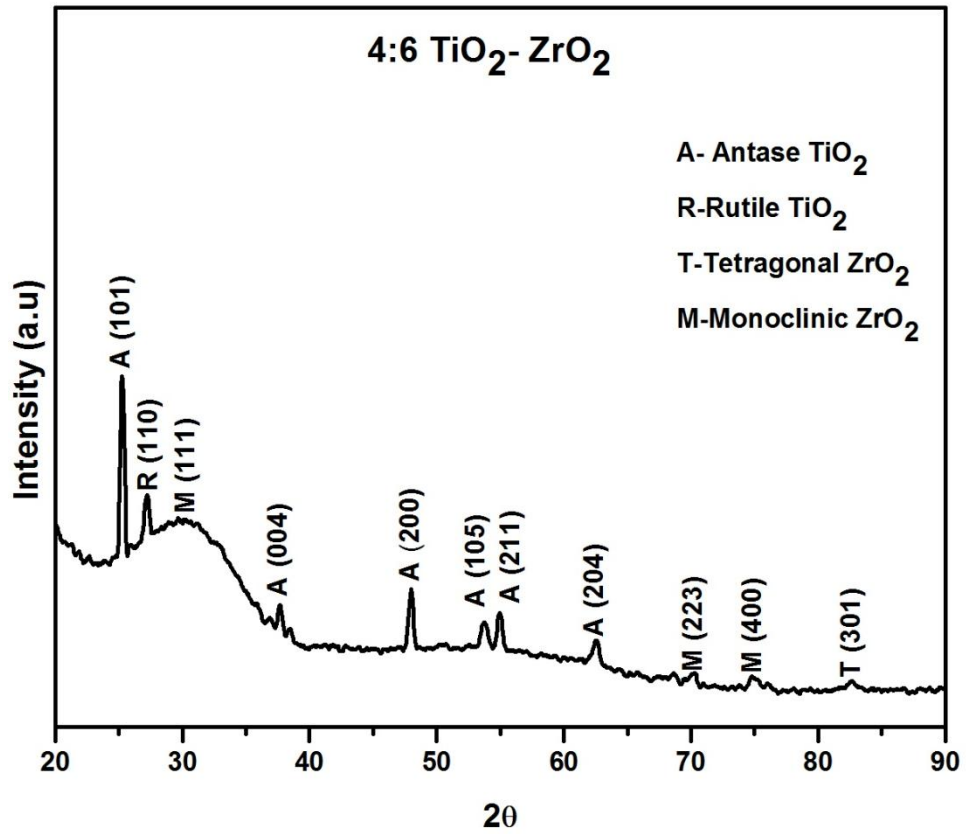


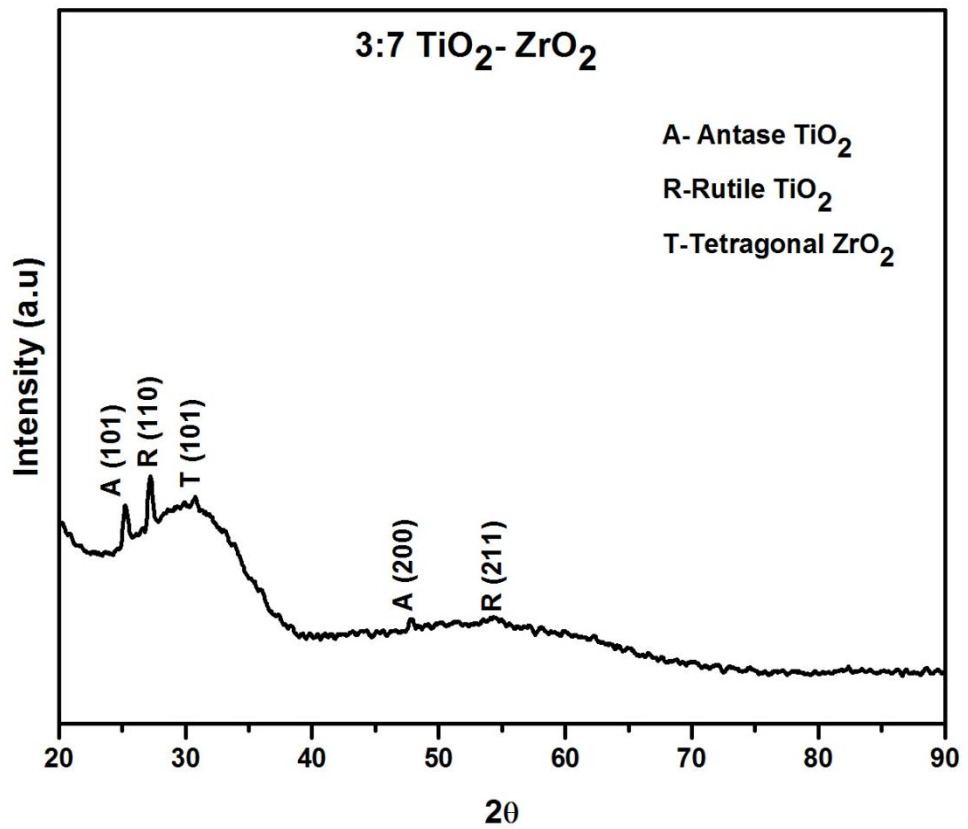
Figure 3: XRD pattern of sample 6:4 TiO₂-ZrO₂ composite

Table 3: Structural parameters of 6:4 TiO₂-ZrO₂ composite

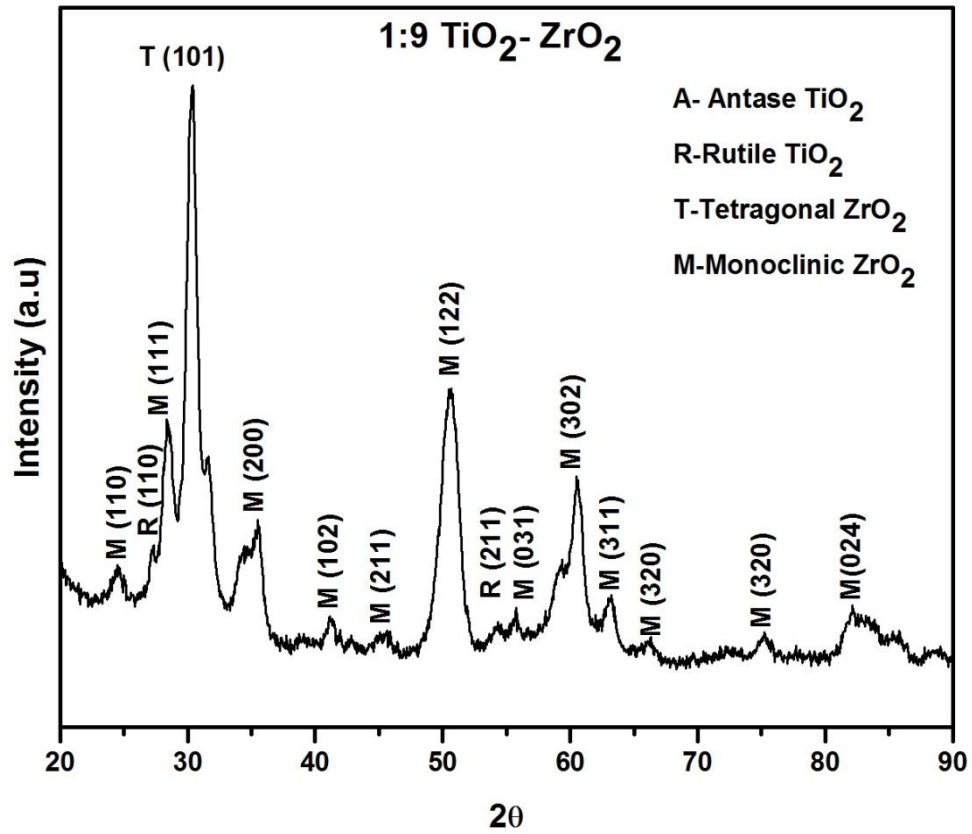
Experimental d values	JCPDS d values	Crystallite size (nm)	Strain (%)	Anatase content (%)
3.51607	3.5200	19.38	0.035	
3.26872	3.2470	24.86	0.025	
3.08052	3.1598	--	--	
2.38322	2.3780	--	--	48.71
1.89497	1.8920	17.75	0.021	
1.7019	1.6999	10.89	0.030	
1.66478	1.6665	14.15	0.023	
1.48427	1.4808	--	--	

Figure 4: XRD pattern of sample 4:6 TiO₂-ZrO₂ compositeTable 4: Structural parameters of 4:6 TiO₂-ZrO₂ composite

Experimental d values	JCPDS d values	Crystallite size (nm)	Strain (%)	Anatase content (%)
3.5229	3.5200	29.99	0.023	52.88
3.2687	3.2470	18.18	0.035	
3.0243	3.1598	--	--	
2.3862	2.3780	23.48	0.019	
1.8949	1.8920	23.39	0.015	
1.7033	1.7968	11.00	0.030	
1.6703	1.6752	18.77	0.017	
1.4842	1.4808	14.30	0.020	

Figure 5: XRD pattern of sample 3:7 TiO₂-ZrO₂ compositeTable 5: Structural parameters of 3:7 TiO₂-ZrO₂ composite

Experimental d values	JCPDS d values	Crystallite size (nm)	Strain (%)	Anatase content (%)
3.5160	3.5200	17.74	0.038	
3.2805	3.2470	21.23	0.030	
2.9134	2.9529	--	--	41.99
1.8949	1.8920	--	--	
1.6816	1.6874	--	--	

Figure 6: XRD pattern of sample 1:9 TiO₂-ZrO₂ compositeTable 6: Structural parameters of 1:9 TiO₂-ZrO₂ composite

Experimental d values	JCPDS d values	Crystallite size (nm)	Strain (%)	Anatase content (%)
3.6290	3.6323	6.78	0.105	
3.2628	3.2400	8.53	0.067	
3.1443	3.1598	4.09	0.121	
1.8001	2.9529	5.44	0.065	-
1.6859	1.6874	8.30	0.036	
1.6469	1.6457	9.03	0.031	
1.5284	1.5381	8.12	0.030	

Table 7: Structural parameters of TiO₂-ZrO₂ composite

Sample	Crystallite Size (nm)	Anatase Content%	Strain	Lattice Parameters			
				Anatase		Rutile	
				a	C	a	c
9:1 TiO₂-ZrO₂	7.36	57.94	0.067	3.78	9.56	4.63	2.89
7:3 TiO₂-ZrO₂	15.28	62.04	0.040	3.78	9.53	4.62	-
6:4 TiO₂-ZrO₂	17.41	48.71	0.027	3.79	9.83	4.64	2.98
4:6 TiO₂-ZrO₂	19.88	52.88	0.023	3.78	9.54	4.62	-
3:7 TiO₂-ZrO₂	19.4	41.99	0.034	3.78	9.57	4.64	2.87
1:9 TiO₂-ZrO₂	6.97	Rutile	0.065	-	-	4.61	2.92

Some of the general features of the patterns are mentioned below.

The highest peak in four of the six samples with TiO₂ content up to 40% has been found to be for the (101) plane of Anatase phase. The Anatase phase content in all these samples is substantial. This is significant as the Anatase phase gives better results for DSSC. The results are supported by other studies [5].

A hump like feature around 2 θ value of 30.5⁰ remains common in all samples with more than 30% ZrO₂ content suggesting some amorphicity in the samples. However there is a Tetragonal phase (101) of ZrO₂ around that which becomes most prominent in the sample with 90% ZrO₂.

Other peaks including the one corresponding to Anatase phase (200) of TiO₂ is also seen in all samples with high content of TiO₂, which results into a higher content of Anatase phase.

The peak at 2θ value of 47.95° is the characteristic peak of Anatase phase of TiO₂ but as the ZrO₂ concentration reaches to 90% this peak vanishes and a new peak at 2θ value of 50.65° which represents crystalline plane (110) of Monoclinic phase of ZrO₂ appears. This is clearly visible in XRD pattern of 1:9 TiO₂-ZrO₂ composite.

A broad peak at 2θ value of 54.5° has been observed in XRD pattern of only 9:1 TiO₂-ZrO₂ composite. This peak corresponds to crystalline plane (211) of Rutile phase of TiO₂.

Few more peaks corresponding to monoclinic phase of ZrO₂ have been observed at 2θ values of 35.50° , 50.65° , 55.75° and 60.5° in XRD pattern of 1:9% TiO₂-ZrO₂ composite.

The features are generally broad, which suggests the formation of material in nanocrystalline form. The calculation of crystallite size using Scherrer formula gives the crystallite size between 7 to 20 nm.

The peaks correspond to the various known phases of TiO₂ as well as ZrO₂ and match with the standard JCPDS values. Hence the occurrence of the individual oxides remains in their pure form in the samples. No other significant peaks are observed.

Table 7 shows different structural parameters of TiO₂-ZrO₂ composites derived from XRD results. The average crystallite size of all the samples lies between 6.97 nm and 19.88 nm. The smallest crystallite size has been observed for the samples 1 and 7. The highest lattice strain has been also observed for the same samples. This might be due to the smaller crystallite size [6, 7]. For higher content of TiO₂ and ZrO₂ the crystallite size increases but is restricted below 20 nm.

The Anatase mass fraction varies as the concentration of ZrO₂ varies. The highest Anatase mass fraction of 62.04% has been observed for 7:3 TiO₂-ZrO₂ composite. Addition of ZrO₂ does not adversely affect formation of Anatase phase but as ZrO₂ concentration increases from 30 to 90 the Anatase content decreases and reaches to 35.91%, which looks logical.

The lattice parameters have been calculated only for the Anatase and Rutile phases as they are the significant parameters from the utility point of view. The Anatase phase, as stated earlier is important for the use of TiO₂ as the electrode material for DSSC. The calculation has been done only for the available planes of phases in the particular samples. The values of these parameters have been by and large found to be uniform, which suggests consistency in the formation of these phases.

Although most of the studies conducted on TiO₂-ZrO₂ for DSSC electrode have a lower content of ZrO₂, this study attempts to investigate higher content of ZrO₂ (30%) to study the possible role of ZrO₂ in the mixed oxide as the electrode. The sample with 30% ZrO₂ also shows a higher Anatase content, which is another reason why TiO₂-ZrO₂ sample in the ratio of 7:3 was considered for further study as an electrode.

5.3.2 UV-Visible Spectroscopy

The optical properties of prepared samples were investigated by UV-Visible absorption spectra. The absorption spectra were recorded on Thermo Fisher Scientific make Evolution 600 Spectrophotometer in the wavelength range of 200-900 nm. The optical bandgap was evaluated by Tauc's plot. The absorption spectra and relative Tauc's plot are shown in figure 7 to figure 12.

The different optical parameters calculated from UV-Visible absorption spectra are given in Table 8.

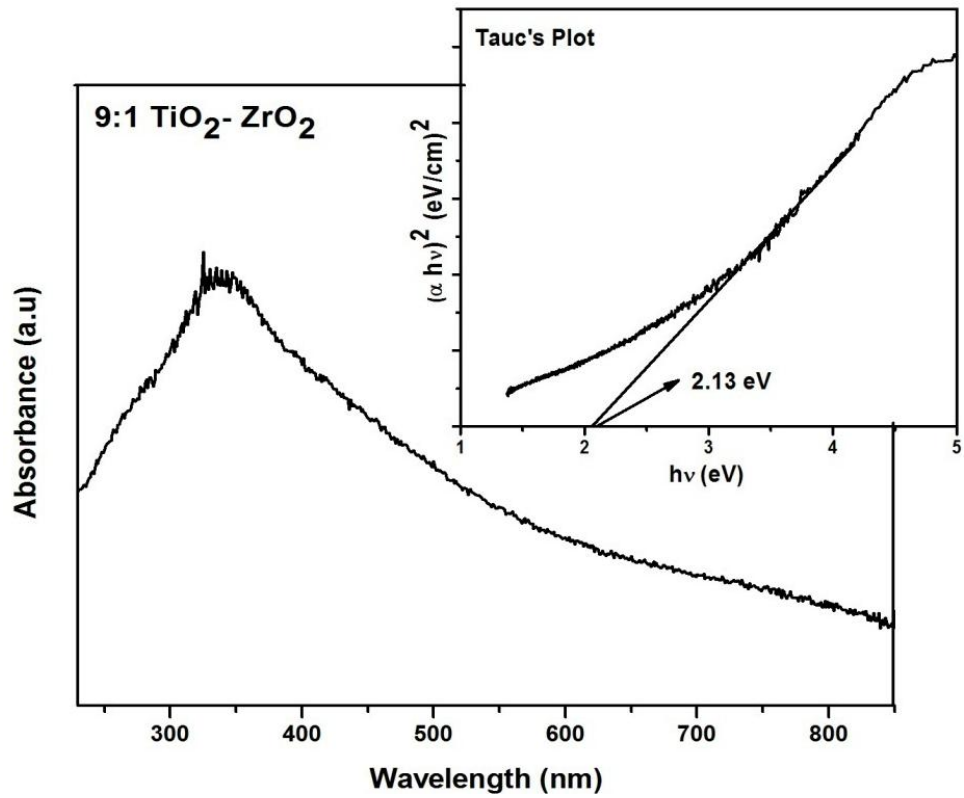


Figure 7: Absorption spectrum and Tauc's plot for 9:1 TiO₂-ZrO₂ composite

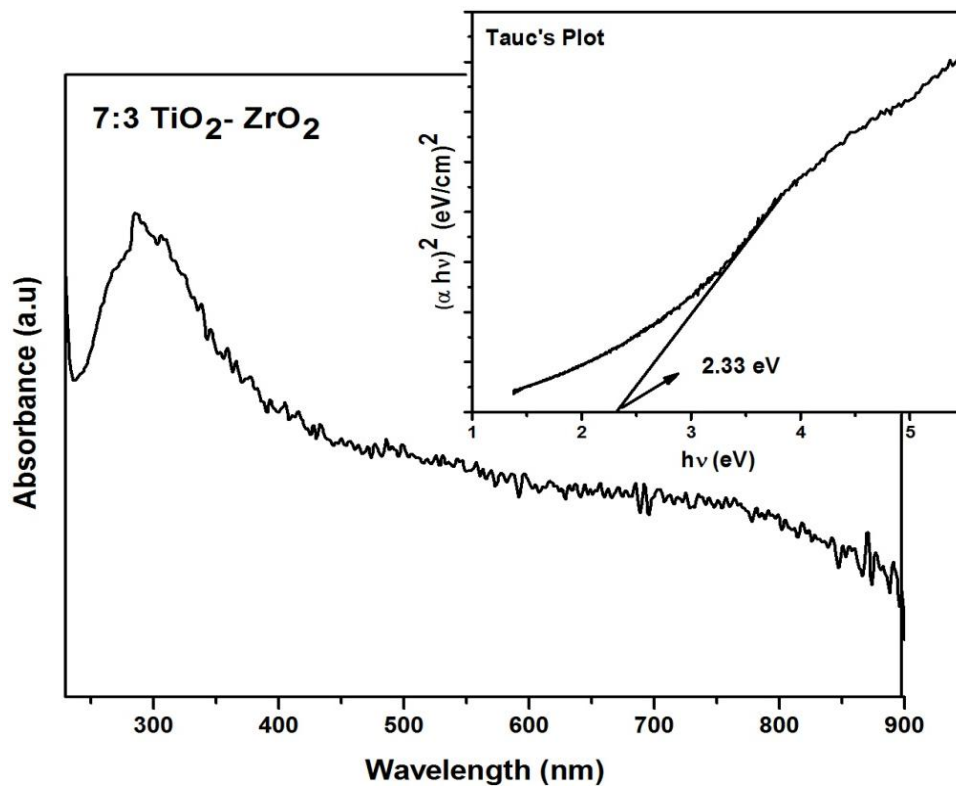


Figure 8: Absorption spectrum and Tauc's plot for 7:3 TiO₂-ZrO₂ composite

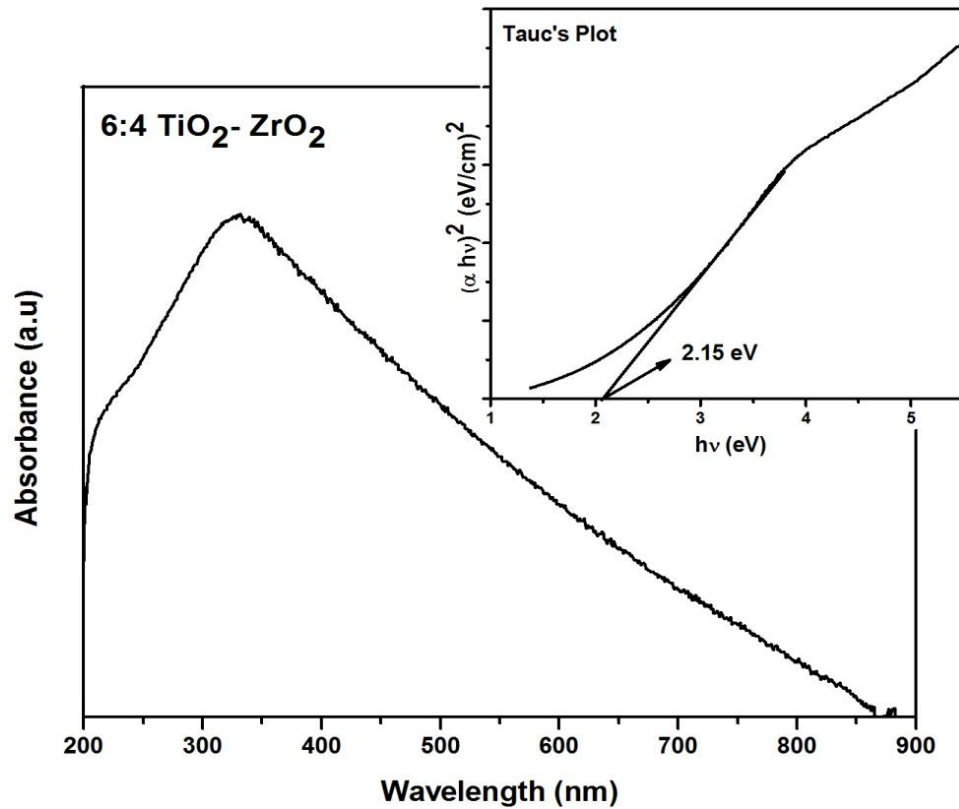


Figure 9: Absorption spectrum and Tauc's plot for 6:4 TiO₂-ZrO₂ composite

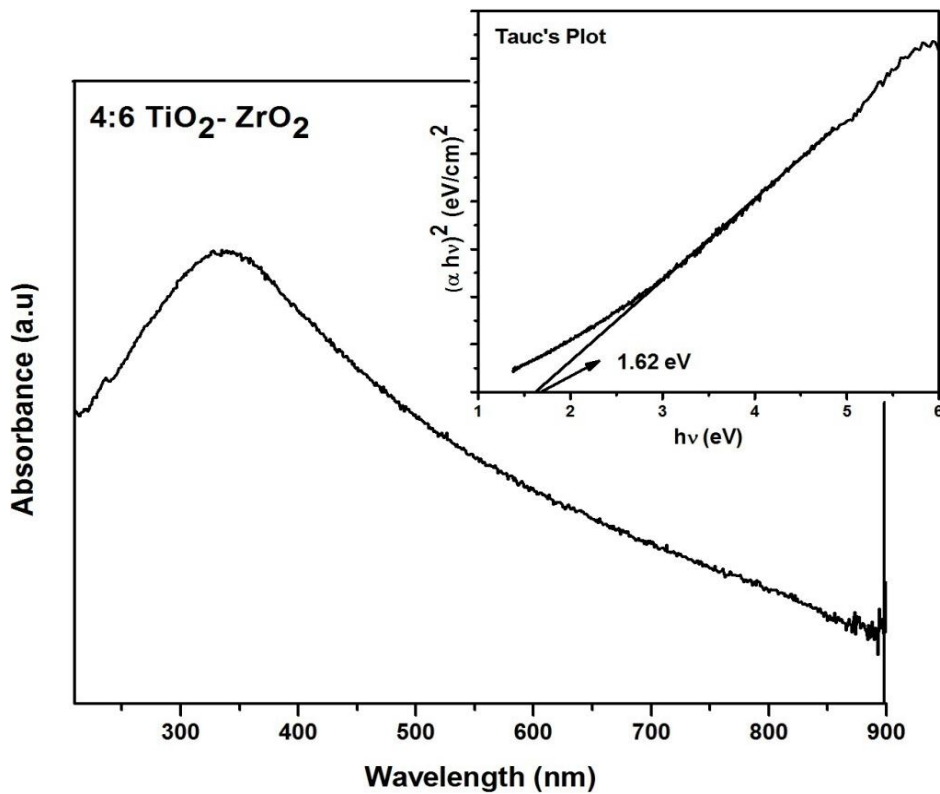


Figure 10: Absorption spectrum and Tauc's plot for 4:6 TiO₂-ZrO₂ composite

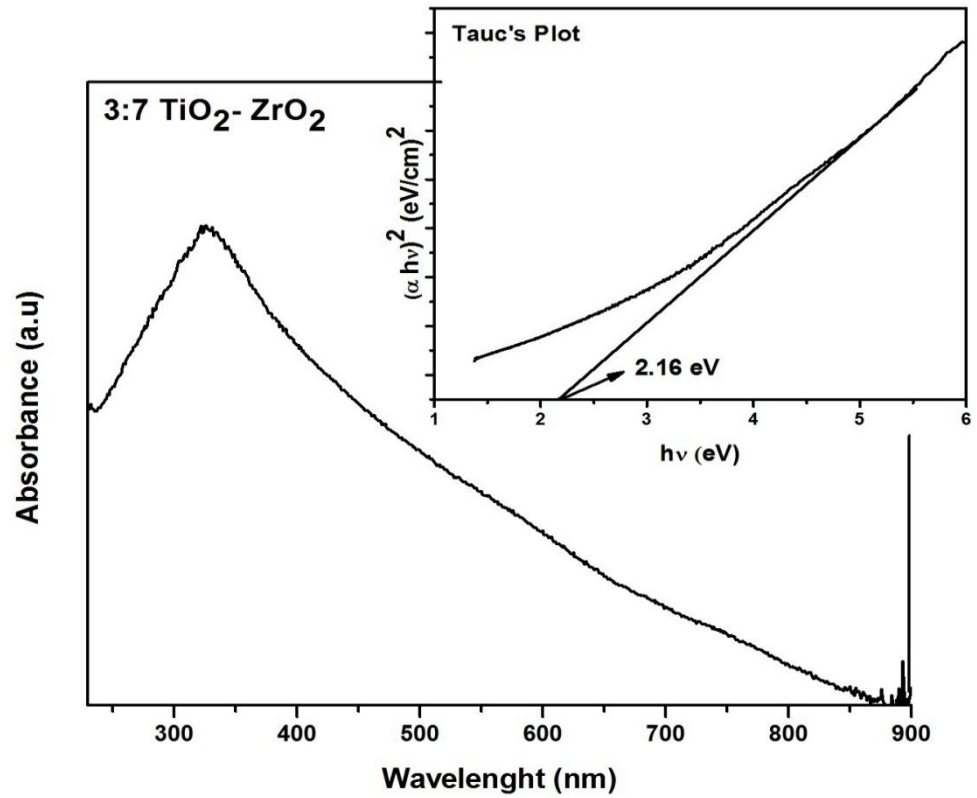


Figure 11: Absorption spectrum and Tauc's plot for 3:7 TiO₂-ZrO₂ composite

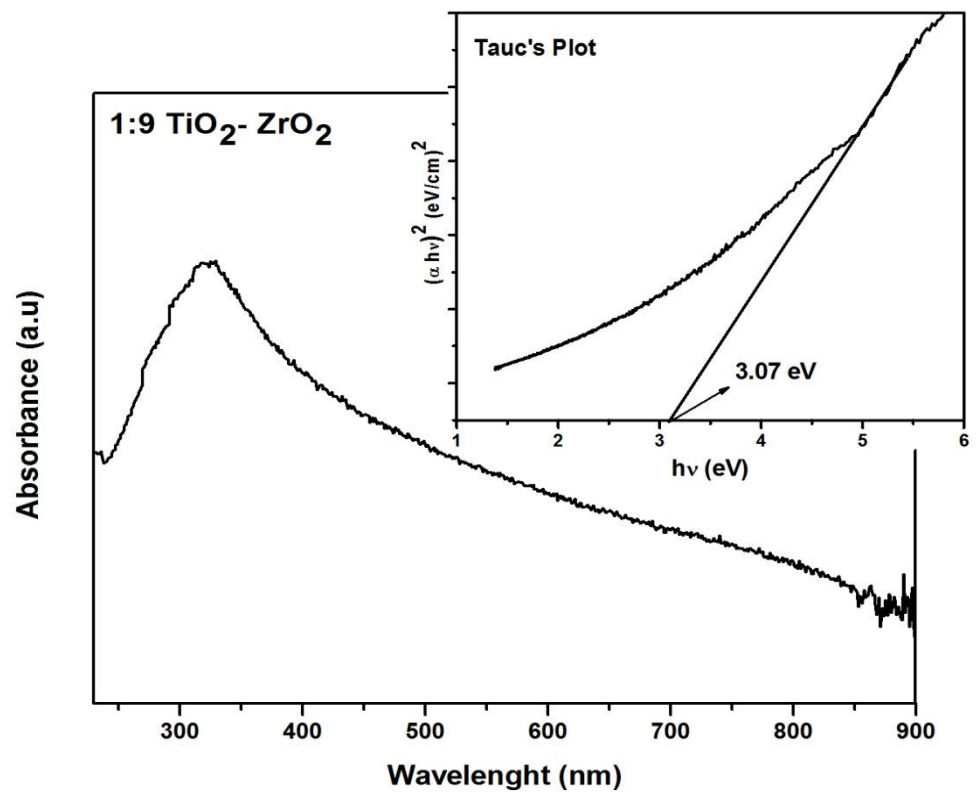


Figure 12: Absorption spectrum and Tauc's plot for 1:9 TiO₂-ZrO₂ composite

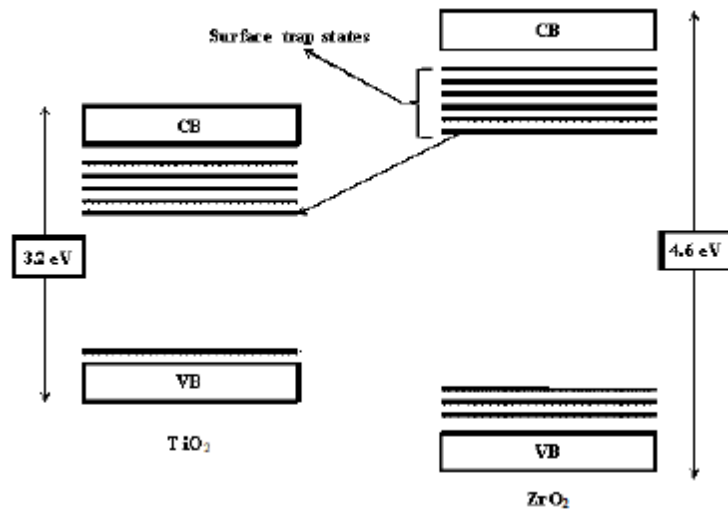
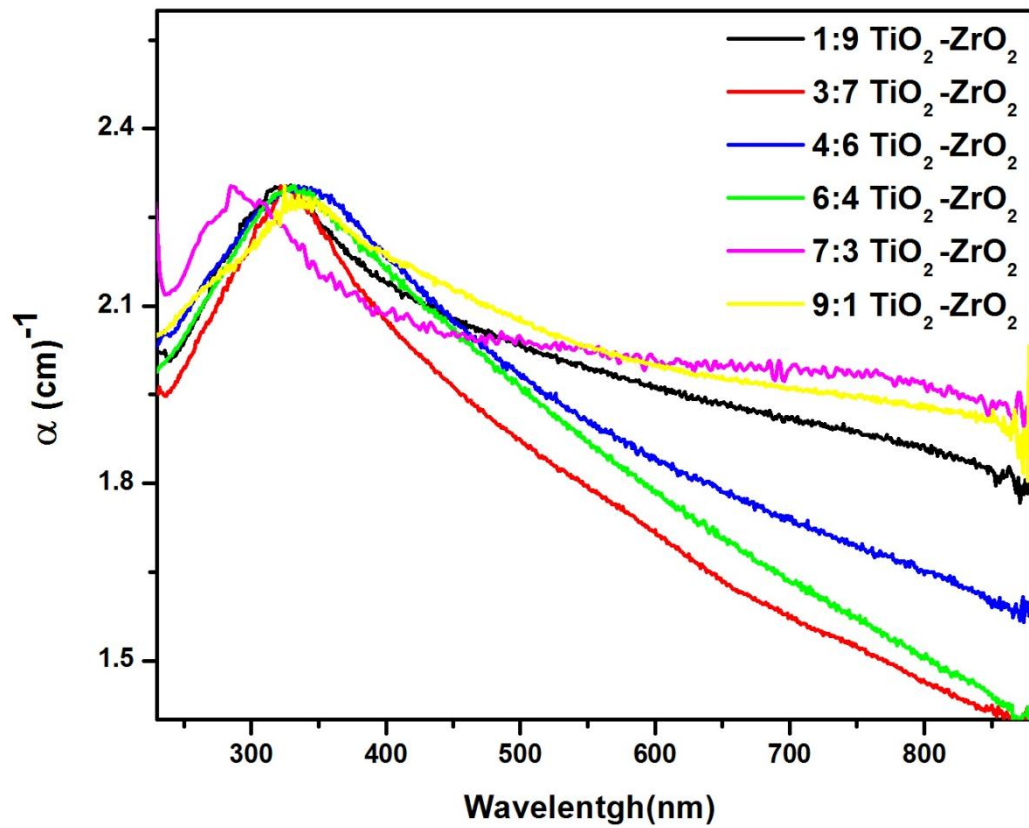
Figure 13: Energy level diagram for TiO₂-ZrO₂

Figure 14: Variation of absorption coefficient with wavelength

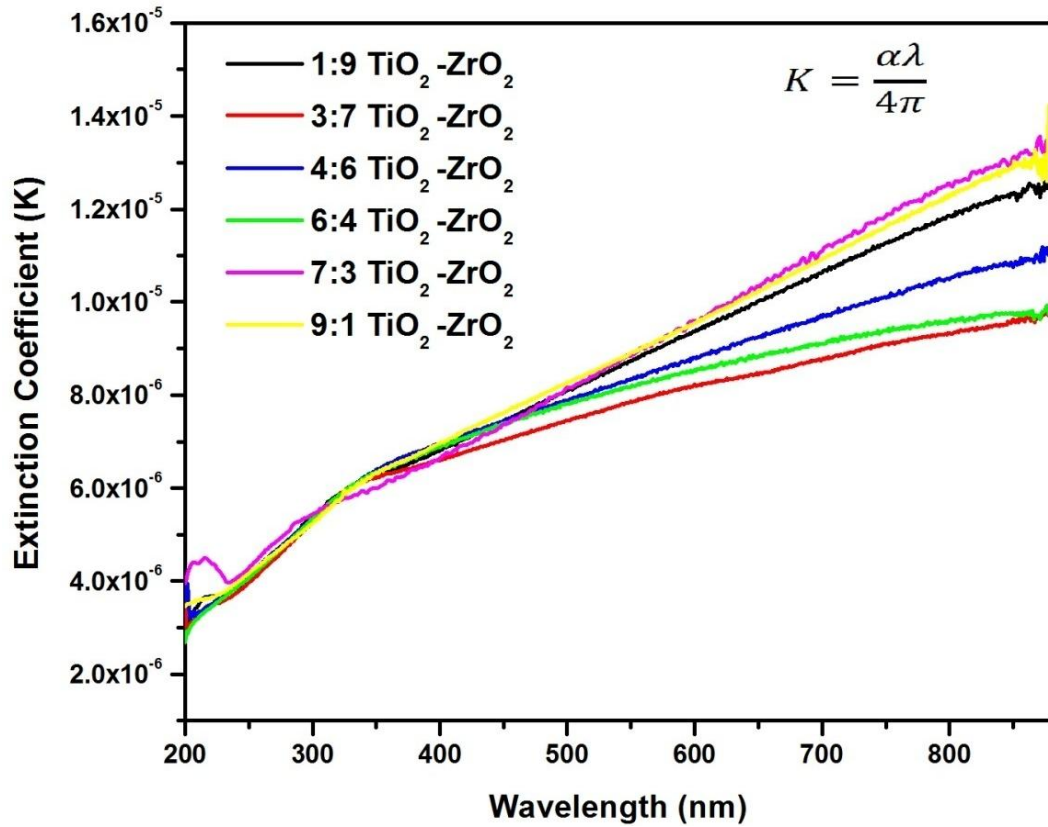


Figure 15: Variation of absorption coefficient with wavelength

Table 8: Different optical parameters of TiO₂-ZrO₂ samples

Sample	Peak Absorption (nm)	Bandgap (eV)	Refractive Index
9:1 TiO ₂ -ZrO ₂	337	2.13	2.63
7:3 TiO ₂ -ZrO ₂	286	2.33	2.56
6:4 TiO ₂ -ZrO ₂	328	2.15	2.62
4:6 TiO ₂ -ZrO ₂	339	1.62	2.87
3:7 TiO ₂ -ZrO ₂	324	2.16	2.62
1:9 TiO ₂ -ZrO ₂	326	3.07	2.34

The following observations can be made from the results.

The peak absorbance of all the samples is between 320 to 340 nm except sample 2 with 70% TiO₂ and 30% ZrO₂ whose peak absorption is at lower wavelength. Thus, this sample can absorb at lower ultraviolet wavelengths.

The absorption coefficient of the samples, which indicates the amount of radiation absorbed in the sample, is given in Figure 14. It shows that the sample 2 again has a higher value of the coefficient in the entire visible range as well. This continues upto near infrared.

Figure 15 shows the variation of extinction coefficient with wavelength. The curves for extinction coefficient which signifies the combination of energy absorbed and energy scattered also shows the same trend.

The refractive index of the samples also varies in a small range except the sample dominated by ZrO₂ i.e. the last sample. Hence the density and transparency of the samples are almost same.

The bandgap of the samples were calculated using Tauc's plot. The sample with 7:3 ratio of TiO₂-ZrO₂ has a relatively high bandgap of 2.33 eV. Sample 4 shows the lowest bandgap. However the sample is not purely crystalline. The bandgap of sample with 90% ZrO₂ has been found to be 3.07 eV. For the other three samples, the bandgap is almost same.

The bandgap of pure TiO₂ is 3.2 eV while that of pure ZrO₂ is 4.6 eV. Their mixture might result into a bandgap picture given in the figure 20.

The modification in the bandgap may be attributed to the sub-bandgap absorptions [8, 9]. These sub band gap absorption may arise from surface states of

the TiO₂-ZrO₂ material. These surface states are surface localized electronic states within the material bandgap, involving complex species such as dangling bonds, defects and atoms adsorbed on the surface [10, 11].

5.4 Conclusion

Based on the structural properties of the sample obtained from the XRD results and the optical properties of the samples from UV-Visible analysis, sample 2 with 70% TiO₂ and 30% ZrO₂ has been found suitable as the mixed oxide electrode material for further studies.

References

- [1] N.I.K uznetsova, L.I.K uznetsova, L.G.Detushe va, V.A. Likholobov, G.P .Pez, and H.Cheng, *J. Mol. Catal. A*, 2000, 161, 1.
- [2] M.Caldararu, M.F .Thomas, J.Bland, and D.Spranceana, *Appl. Catal. A*, 2001 209, 383.
- [3] X. Fu, L.A. Clark, Q. Yang, M.A. Anderson, *Environ. Sci. Technol*, 1996, 30, 647–653.
- [4] Athapol Kitiyanan, Supachai Ngamsinlapasathian, Soropong Pavasupree, Susumu Yoshikawa, *Journal of Solid State Chemistry*, 2005, 178, 1044–1048
- [5] Htet Htet Nwe, Yin Maung Maung, Than Than Win and Ko Ko Kyaw Soe, *Journal of Science (JOS)*, 2012, 3, 197.
- [6] Biswajit Choudhury and Amarjyoti Choudhury, *International Nano Letters* 2013, 3, 1.
- [7] M. E. Manriquez, M. Picquart, X. Bokhimi, T. Lopez, P. Quintana, and J. M. Coronado, *J. Nanosci. Nanotechnol*, 2008, 8, 1.
- [8] W. Tong-Shun, W. Kai-Xue, Z. Lu-Yi, L. Xin-Hao, W. Ping, W. De-Jun, and Jie-Sheng Chen *J. Phys. Chem. C*, 2009, 113, 9114–9120
- [9] X.Bokhimi, A.Morales, O.No varo, M.Portilla, T.Lopez, F.Tzompantzi, and R.Gomez, *J. Solid State Chem.* 1998, 135, 28.
- [10] L. Kronik, Y. Shapira, *Surf. Interface Anal*, 2001, 31, 954–965.
- [11] L. Kronik, Y. Shapira, *Surf. Sci. Rep*, 1999, 37, 1–206.